

# Mechanism of ionospheric descent prior to intense earthquakes by electrostatic coupling with an electrically charged fractured layer

Akira Mizuno, Minghui Kao, Ken Umeno\*

Department of Applied Mathematics and Physics, Graduate School of Informatics,  
Kyoto University, Kyoto, Japan

\* Corresponding author: [umeno.ken.8z@kyoto-u.ac.jp](mailto:umeno.ken.8z@kyoto-u.ac.jp) (Ken Umeno)

Received: 1 March 2024

Revised: 20 March 2025

Accepted: 11 April 2025

Published online: 16 April 2025

## Abstract

Ionospheric descent has been observed prior to intense earthquakes. Changes in the velocity of Medium-Scale Traveling Ionospheric Disturbances (MSTID) have also been reported, leading to various discussions about the electromagnetic coupling between the Earth's crust and the ionosphere. We previously reported that during pre-seismic fracturing of the crust, water penetrates the fractured layer in a high-temperature, high-pressure supercritical state. Due to sudden pressure changes during penetration, nanoparticles can be generated from ions dissolved in the supercritical water. Additionally, due to the low conductivity and high temperature of the supercritical water, electron emission from nanoparticles can occur, resulting in their positive charging. When the fractured layer becomes charged, the Earth's surface potential changes, affecting the electric field strength between the Earth's surface and the lower ionosphere. By assuming that the charged fractured layer attracts the ionosphere, we estimated the time constant of ionospheric descent, finding that the calculated value closely matches the observed descent time constant. This suggests that electrostatic capacitive coupling between the charged fractured layer and the ionosphere may be responsible for the ionospheric anomalies observed before intense earthquakes.

**Keywords:** 2024 Noto earthquake, supercritical water, electric field, ionospheric descent, ionogram.

## 1. Introduction

Prior to intense earthquakes, crustal fractures can be filled by supercritical water containing dissolved ions, leading to nanoparticle formation [1, 2]. High temperatures due to geothermal heating and friction cause thermionic electron emission, positively charging the nanoparticles [3]. Since supercritical water has low electrical conductivity, the fractured layer can be regarded as a capacitor [2, 4].

Anomalies such as change of total electron content, TEC, and ionospheric descent [5, 6], changes in MSTID velocity [7, 8], and electromagnetic wave emissions [9] have been observed before intense earthquakes. We hypothesize that charged fractured layers may be responsible for these phenomena. Previously, we reported on the capacitance and electrostatic energy of fractured layers [1]. In this study, we estimate the time constant of ionospheric descent caused by electrostatic coupling with a charged fractured layer. It should be noted that our hypothesis excludes space-weather induced disturbances.

## 2. Electrostatic coupling of the charged fractured layer and the ionosphere

Recent geological surveys near large earthquake epicenters have revealed that fault gouges contain smectite, a slippery mineral that may retain absorbed water [10]. Prior to intense earthquakes, crustal water infiltrates the fractured layer as supercritical water, expanding and generating nanoparticles [4]. Due to a decrease in the ion product of water upon expansion, nanoparticles are generated. Frictional heating in geothermally high-

temperature areas induces thermionic emission, resulting in positive charging of the fractured layer. The interlayer voltage of the charged fractured layer, estimated based on micro-gap spark breakdown experiments, is approximately  $V_s \approx 300 \text{ V}$  [11]. This electrical breakdown may generate electromagnetic waves [9, 12].

Crustal fracturing before an intense earthquake often occurs in multiple stages, culminating in a major rupture [13]. To calculate the electrostatic energy of the fractured layer, we consider a single crustal fracture parallel to the Earth's surface.

Assuming the fractured layer thickness is  $10^{-5} \text{ m}$ , and the relative permittivity within the layer is 5.0, the capacitance per unit area, charge amount, and electrostatic energy are:

$$\text{Electrostatic capacitance } C_0 : \quad 4.43 \times 10^{-6} \text{ F m}^{-2} \quad (1)$$

$$\text{Charge amount } Q_0 : \quad 1.3 \times 10^{-3} \text{ C m}^{-2} \quad (2)$$

$$\text{Electrostatic energy } W_0 : \quad 2.0 \times 10^{-1} \text{ J m}^{-2} \quad (3)$$

A charged fractured layer generates an electric field,  $E_z$ , between the Earth's surface and the ionosphere, superimposing onto the global circuit (Fig. 1). This perturbation terminates at the lower ionospheric boundary due to the short Debye length of the ionosphere [14]. At this boundary, diffusive electrons are extracted by  $E_z$  and recombine with neutral molecules or positive ions, forming space charges that attenuate  $E_z$ . As electrons are extracted, upper-layer plasma is pulled downward to maintain electrical neutrality.

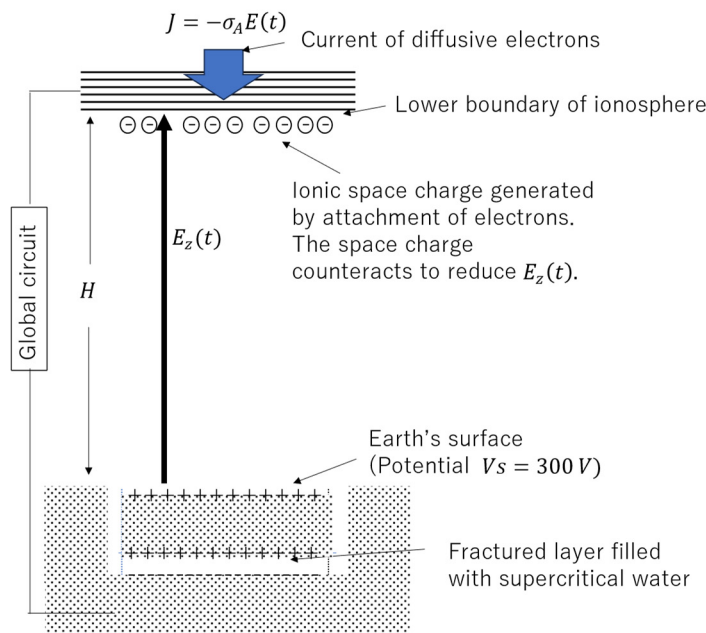


**Fig. 1.** Schematic diagram of the effect of charged fractured layer filled with supercritical water in the crust to cause ionospheric descent.

The attenuation of  $E_z$  occurs through the following paths: (a) charge dissipation within the supercritical fractured layer, (b) discharge through the surrounding crust, and (c) generation of space charge under the ionosphere. In paths (a) and (b), the electric field decreases due to the discharge of stored charge, while in (c), the electric field is reduced by the space charge created by electrons flowing out of the lower boundary of the ionosphere. In the following discussion, we assume that the time constants of paths (a) and (b) are long compared to that of ionospheric descent and consider only the attenuation of  $E_z$  caused by path (c).

It has been reported that the ionosphere descends by approximately 20 km before an intense earthquake [6]. Assuming the electron density of the ionosphere,  $N_e = 5 \times 10^{11} \text{ m}^{-3}$ , and the electronic charge  $e = -1.6 \times 10^{-19} \text{ C}$ , the total charge of electrons per unit area contained within a descent distance of  $D = 20 \text{ km}$  is calculated as follows:

$$Q_D = eN_e D = -1.6 \times 10^{-3} \text{ C m}^{-2} \quad (4)$$

This value is close to cancel the charge given in equation (2). If the charge in the fracture,  $Q_0 = 1.3 \times 10^{-3} \text{ C m}^{-2}$  in Eq. (2) is used for the descent,  $D$  could be 16.5 km.

### 3. Estimation of ionospheric descent velocity

Assuming that the electric field generated by the charged fractured layer induces ionospheric descent, we estimate the descent velocity.

The ionospheric conductivity comprises parallel conductivity  $\sigma_0$ , Pedersen conductivity  $\sigma_P$ , and Hall conductivity  $\sigma_H$ . As the height decreases to near 100 km, all conductivities decrease [11]. The apparent conductivity of the lower ionosphere boundary,  $\sigma_A$ , is unknown and estimated as follows.

The electric field  $E_z$  terminates at the lower ionospheric boundary due to the short Debye shielding length [12], extracting diffusive electrons. The extracted electrons attach to neutral molecules or positive ions, forming low-mobility negative space charges that reduce  $E_z$  over time. Therefore,  $E_z$  can be noted as  $E_z(t)$ . The electrons of upper-ionosphere diffuse downward to compensate for the shortage of electrons at the lower boundary. The descent of electrons in the dense part of the plasma will be followed by positive ions, causing the ionospheric descent observed in ionograms.

The electron current density,  $J(t)$ , extracted by  $E_z(t)$  depends on the apparent conductivity  $\sigma_A$  of the boundary. The extracted current density,  $J(t)$ , is given by

$$J(t) = -\sigma_A E_z(t) \quad (5)$$

The apparent conductivity,  $\sigma_A$ , is not known. Therefore, we estimate  $\sigma_A$  from the observed descent velocity of the ionosphere.

Fig. 2 shows the time variation of the height,  $H$  of ionosphere (F-layer) measured using an oblique (Yamagawa-Wakkanai) ionosonde observation during the Noto Peninsula earthquake (M7.6) on January 1, 2024, at 16:10 JST. The original recorded data have been provided by NICT (National Institute of Information and Communications Technology) [15]. Using this oblique ionogram observation between Wakkanai (transmitter) and Yamagawa (receiver) in Japan, we analyze time variations in ionospheric height around the Noto Peninsula [16]. As reported in ref.16, the first-hop reflection point of this oblique ionogram is slightly north of Noto-Peninsula and close to the epi-center of the earthquake.

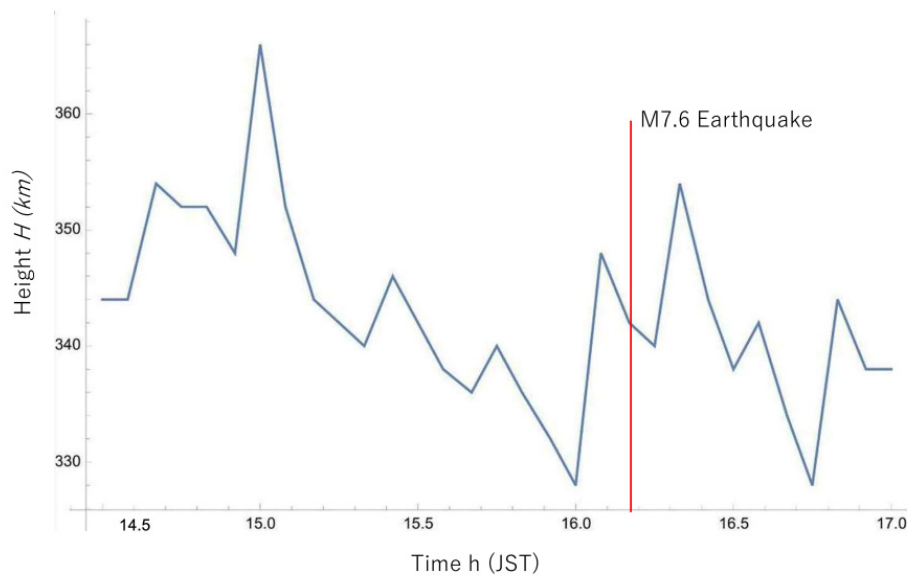


**Fig. 2.** Height of F-layer of the ionosphere measured using an oblique ionogram (Wakkanai transmitter -Yamakawa receiver oblique data provided by NICT [15]), prior to an intense earthquake of M7.6 at Noto Peninsula, Japan, on Jan. 1, 2024.

Fig. 3 shows an oblique ionogram one hour prior to the main shock of the Noto Peninsula earthquake. The signal emitted from Wakkanai, Hokkaido, Japan, has been received at Shionomisaki Wind Effect Laboratory, Wakayama, a research facility of Kyoto University. The sounding point of the oblique ionogram is about 250 km northeast of Noto peninsula. The data, published in 2024 [17], also showed the decrease of the height of ionosphere.

From  $T = 15:00$  h to  $15:10$  h (JST), during 0.1 h (360 sec),  $H$  decreased from 366.0 km to 351.6 km, corresponding to a descent of 14.4 km. During this period, the averaged descent velocity is read to be  $v_{ave} = 40 \text{ m s}^{-1}$ .

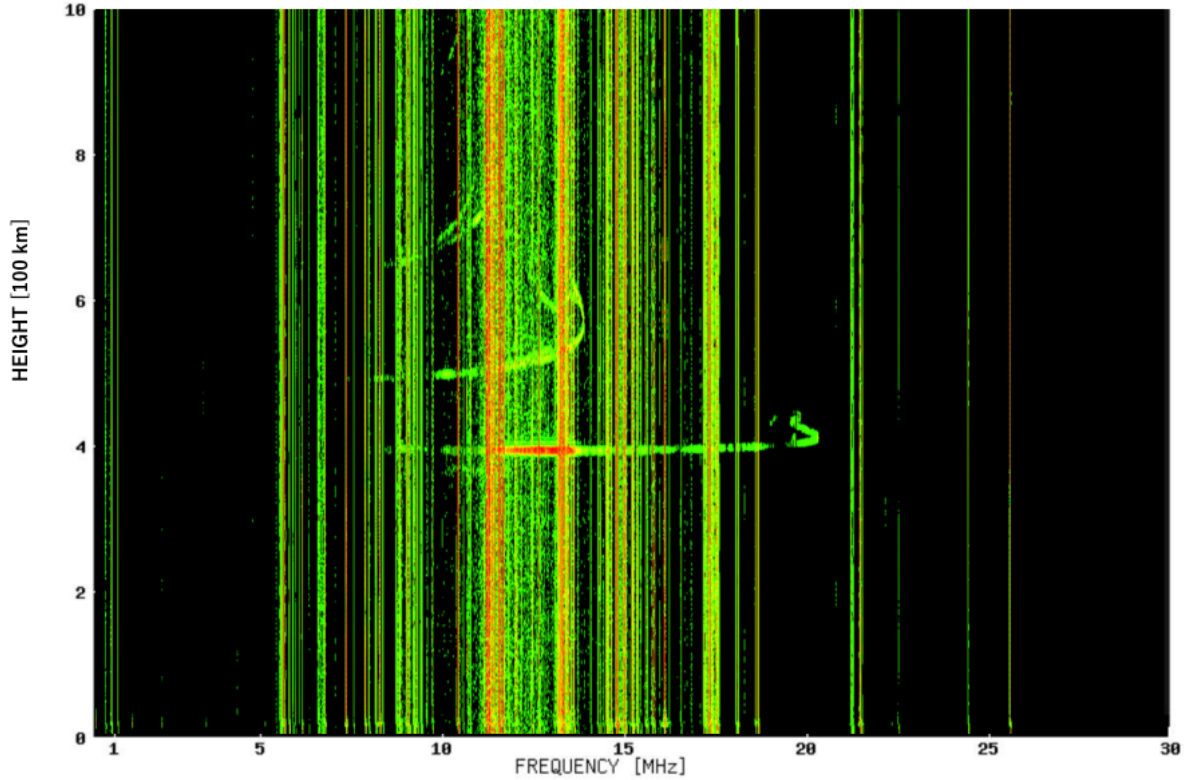


**Fig. 3.** An oblique ionogram (Wakkanai-Shionomisaki) at 15:00 JST, January 1, 2024, 1hour 10 min. prior to Noto Peninsula Earthquake [17]. The signal emitted from Wakkanai, Hokkaido, was received at the Shionomisaki Wind Effect Laboratory Kyoto University, Wakayama. The location of the sounding point (first-hop reflection point) is about 250 km northeast of the epi-center.

To minimize reading errors from the graph, we assume the height  $H$  being an exponential decay function with time constant  $\tau$ , and use the relationship that the slope at  $t = 0$  is  $\sqrt{e}$  times the slope at  $t = \tau/2$ . From the graph in Fig. 1,  $\tau$  can be estimated to be between 360 and 720 sec. The slope at  $t = 360$  s ( $40 \text{ m s}^{-1}$ ) is regarded as the slope at  $t = \tau/2$ . Then the initial ionospheric descent velocity, immediately after the start of this descent, is estimated to be  $v(0) = 66 \text{ m s}^{-1}$ .

Given an electron density at this height,  $N_e = 5 \times 10^{11} \text{ m}^{-3}$ , the charge transported by electrons in the first 1 second (current density) is:

$$J(0) = e N_e v(0) = -5.3 \times 10^{-6} \text{ A m}^{-2} \quad (6)$$

The initial electric field  $E_z(0)$  at  $H = 100$  km is:

$$E_z(0) = 3.0 \times 10^{-3} \text{ V m}^{-1} \quad (7)$$

The electrons are extracted from the boundary by  $E_z(0)$  to constitute the current. Therefore, the apparent conductivity can be obtained from the following relation.

$$J(0) = -\sigma_A E_z(0), \quad \sigma_A = 1.8 \times 10^{-3} \text{ S m}^{-1} \quad (8)$$

The extracted electrons form negative space charge and reduce  $E_z(t)$ .

$$\frac{dQ(t)}{dt} = J(t) = -\sigma_A E_z(t) \quad (9)$$

$$C_0 H E_z(t) = Q_0 - \int_0^t \sigma_A E_z(t) dt \quad (10)$$

Assuming:  $C_0 = 4.4 \times 10^{-6} \text{ F m}^{-2}$ ,  $V_s \approx 300 \text{ V}$ ,  $Q_0 = 1.3 \times 10^{-3} \text{ C m}^{-2}$ , then

$$E_z(t) = E_z(0) \exp(-t/\tau) \quad (11)$$

$$E_z(0) = 3.0 \times 10^{-3} \text{ V m}^{-1}, \quad \tau = C_0 H / S = 2.5 \times 10^2 \text{ sec.}$$

$$J(t) = -\sigma_A E_z(t) = -5.3 \times 10^{-6} \exp\left(-\frac{t}{2.5 \times 10^2}\right) \text{ A m}^{-2} \quad (12)$$

The time constant of  $\tau = 2.5 \times 10^2 \text{ sec}$  is close to the observed values.

The descending velocity,  $v(t)$

$$v(t) = J(t) / e N_e = 66 \exp\left(-\frac{t}{2.5 \times 10^2}\right) \text{ m/sec} \quad (13)$$

Descending distance,  $D(t)$

$$D(t) = \int_0^t v(t) dt = 16.5 \times 10^3 \left\{ 1 - \exp\left(-\frac{t}{2.5 \times 10^2}\right) \right\} \text{ m} \quad (14)$$

We have proposed an electrostatic coupling model in which the electric field generated by a charged fractured layer induces ionospheric descent. This proposed mechanism is summarized as follows:

The electric field from the Earth's surface to the ionosphere is terminated at the lower boundary of ionosphere, because the Debye length is very small [14]. Assuming that the charge density of both electrons and positive ions in the lower ionosphere are  $3 \times 10^{11} \text{ m}^{-3}$ , then the Debye length is approximately  $2 \times 10^{-2} \text{ m}$ .

Across the lower boundary, highly diffusive electrons are drawn out by the electric field. Then, electrons in the upper-layer diffuse downward to maintain charge neutrality. Positive ions also follow the descending flow of electrons. The extracted electrons attach to neutral molecules or positive ions to form negative space charge having low mobility. In this way, the negative space charge counteracts the terminating electric field generated by the charged fractur in the crust.

The current flowing across the lower boundary determines the ionospheric descent velocity. However, since the electrical conductivity of the boundary layer is unknown, we estimated it by back-calculating from the observed ionospheric descent velocity obtained from the ionogram shown in Fig. 2.

1 hour prior to the earthquake, the observed ionospheric height changed as follows.

- $T = 15.00 \text{ h}$  to  $T = 15.20 \text{ h}$ ,  $H = 366 \text{ km}$  to  $H = 340 \text{ km}$
- $T = 15.40 \text{ h}$  to  $T = 15.70 \text{ h}$ ,  $H = 346 \text{ km}$  to  $H = 336 \text{ km}$
- $T = 15.75 \text{ h}$  to  $T = 16.00 \text{ h}$ ,  $H = 340 \text{ km}$  to  $H = 328 \text{ km}$

The ionosphere exhibited a stepwise descent. The maximum descent observed in a single instance was 26 km (from  $H = 366 \text{ km}$  to  $340 \text{ km}$ ). In contrast, a single instance of charging in the fractured layer is estimated to cause an ionospheric descent of up to approximately 16.5 km. However, the maximum descent observed in Fig. 2 exceeds this value. This comparison suggests a possibility that, prior to a major rupture of the crust, the fracturing took place successively and resulted in a step wise accumulation of the charge in the fractured layer.

Additionally, at the moment of major rupture, the ionospheric height increased. If a charged fractured layer undergoes a major rupture, the charged layer could be segmented and could be discharged through surrounding

conductive boundary of each segment. This rapid discharge could lead a sudden change in the electric field to the ionosphere.

It should be noted that the hypothesis of electrostatic coupling excludes space weather -induced variations. Since ionospheric height is constantly fluctuating, to utilize ionospheric descent as a precursor for earthquakes, it is necessary to identify characteristic changes associated with past major earthquakes and find highly correlated anomalous variations.

#### 4. Conclusion

Prior to intense earthquakes, the crust starts fracturing, and the fractured layer could possibly be electrically charged. An electric field is formed between the Earth's surface and the ionosphere. This study examined whether the amount of charge that accumulates in a fracture layer could be sufficient to cause the observed ionospheric descent before an intense earthquake. The proposed mechanism makes it physically possible for ionospheric anomalies to take place. Moving forward, it is believed that detailed observations of ionospheric anomalies should be conducted to verify the hypothesis presented here.

#### Acknowledgment

This research draws upon data provided by WDC for Ionosphere and Space Weather, Tokyo, National Institute of Information and Communications Technology. We would like to express our gratitude to all the people involved in the Kwasan Observatory of Kyoto University for their cooperation in measuring the electric field strength and atmospheric current on the earth's surface.

#### References

- [1] Mizuno A., Kao M., and K. Umeno K., A capacitive coupling model between the ionosphere and a fault layer in the crust with supercritical water, *Int. J. Plasma Environ. Sci. Technol.*, Vol. 18 (1), e01003, 2024.
- [2] Yoko A. Seong G., Tomai T., and Adschiri T., Continuous flow synthesis of nanoparticles using supercritical water: process design, surface control, and nanohybrid materials, *KONA Powder and Particle Journal*, Vol. 37, pp. 28–41, 2020.
- [3] Freund F., Pre-earthquake signals: Underlying physical processes, *J. Asian Earth Sci.*, Vol. 41, pp. 383–400, 2011.
- [4] Ono T., and Inomata H., Supercritical water -properties and applications-, *Oyo Buturi.*, Vol. 80 (10) , pp. 875–880, 2011. (in Japanese)
- [5] M. Hayakawa M, Molchanov O.A., Ondoh T., and Kawai K., Anomalies in the Sub-ionospheric VLF Signals for the 1995 Hyogo-ken Nanbu Earthquake, *J. Phys. Earth*, Vol. 44, pp. 413–418, 1996.
- [6] Heki K., Ionospheric disturbances related to earthquakes," in *Ionosphere Dynamics and Applications*, ed, 2021, pp. 511–526.
- [7] Iwata T., and Umeno K., Preseismic ionospheric anomalies detected before the 2016 Kumamoto earthquake, *J. Geophys. Res.: Space Phys.*, Vol. 122, pp. 3602–3616, 2017.
- [8] Umeno K., Nakabayashi R., Iwata T., and Kao M., Capability of TEC correlation Analysis and Deceleration at Propagation Velocities of Medium-Scale Traveling Ionospheric Disturbances: Preseismic Anomalies before the Large Earthquakes, *Open J. Earthquake Res.*, Vol. 10, pp. 105–137, 2021.
- [9] Nagao T., Enomoto Y., Fujinawa Y., Hata M., Hayakawa M., Huang Q., Izutsu J., Kushida Y., Maeda K., Oike K., Uyeda S., and Yoshino T., Electromagnetic anomalies associated with 1995 Kobe earthquake, *J. Geodynamics*, Vol. 33 (4–5), pp. 401–411, 2002/05/01/ 2002.
- [10] Kimura G., Hamada Y., Yabe S., Yamaguchi A., Fukuchi R., Kido Y., Maeda L., Toczko S., Okuda H., Ogawa N., Morioka H., Ujiie K., and Saffer D., Deformation process and mechanism of the frontal megathrust at the nankai subduction zone, *Geochem. Geophys. Geosystems*, Vol. 23 (4), e2021GC009855, 2022.
- [11] Yamamo Y., Characteristics of breakdown between electrodes with micro-gap in atmosphere, *J. Institute Electrost. Jpn.*, Vol. 36, pp. 146–151, 2012. (in Japanese)
- [12] Uyeda S., Nagao T., and Kamogawa M., Short-term earthquake prediction: Current status of seismo-electromagnetics, *Tectonophysics*, vol. 470, pp. 205–213, 2009/05/29/ 2009.
- [13] Nishikawa T., Ide S., and Nishimura T., A review on slow earthquakes in the Japan Trench, *Progress in Earth and Planetary Science*, Vol. 10, 1, 2023.
- [14] von Engel A., *Electric Plasmas: their nature & uses*, : Taylor & Francis, 1983.
- [15] *Ionosonde observations by NICT in Japan (National Institute of Information and Communications Technology)*. Available: [https://wdc.nict.go.jp/Ionosphere/en/archive/ionog\\_viewer/index.html](https://wdc.nict.go.jp/Ionosphere/en/archive/ionog_viewer/index.html)

- [16] Igarashi K., Tsuchiya T., and Umeno K., Characteristics of anomalous radio propagation before and after the 2011 Tohoku-Oki earthquake as seen by oblique ionograms, *Open J. Earthquake Res.*, Vol. 9, pp. 100–112, 2020.
- [17] Umeno K., (2024, Oblique Ionogram Data Related to 2024 Noto Peninsula Earthquake. Available: <https://repository.kulib.kyoto-u.ac.jp/dspace/handle/2433/287265>